Research Square

Preprints are preliminary reports that have not undergone peer review.
They should not be considered conclusive, used to inform clinical practice,
or referenced by the media as validated information.

Unsupervised Multiomics Integration Identifies Prognostic Subtypes and Druggable Vulnerabilities in Multiple Myeloma

Hamed Bashiri
Komar University of Science and Technology, Kurdistan Regional Government
Siamak Salimy
Hamadan University of Medical Sciences
Hassan Bashiri
Hamedan University of Technology
Saeid Afshar
safshar.h@gmail.com

Hamadan University of Medical Sciences

Article

Keywords: Multiple myeloma, deep learning, autoencoder, multiomics integration, prognostic modeling, survival analysis

Posted Date: June 17th, 2026

DOI: https://doi.org/10.21203/rs.3.rs-9713112/v1

License: This work is licensed under a Creative Commons Attribution 4.0 International License.
Read Full License

Additional Declarations: No competing interests reported.

Abstract

Multiple myeloma (MM) is a clinically and genomically heterogeneous plasma-cell malignancy in which existing risk stratification systems fail to fully capture survival variability. In this study, we developed an unsupervised deep learning–based multiomics integration framework to improve prognostic stratification and identify biologically informed, potentially druggable vulnerabilities. The proposed pipeline integrates transcriptomic, epigenomic, and clinical data via an autoencoder architecture for nonlinear dimensionality reduction and Lasso—Cox proportional hazards regression for feature selection. We analyzed 559 MM patients from the GSE2658 dataset and validated the findings in an independent cohort (GSE4581). Patients were stratified into prognostic subgroups via a hyperparameter-optimized deep autoencoder and unsupervised k-means clustering, followed by differential expression and pathway enrichment analyses. The model identified 30 survival-associated features that robustly separated patients into high- and low-risk groups, with significant survival differences ($p < 0.001$). Differential expression analysis revealed that 268 dysregulated genes were enriched in bone marrow microenvironmental signaling, DNA damage response dysfunction, PI3K–Akt signaling, and metabolic pathways. These findings demonstrate the utility of integrating deep learning with multiomics data to uncover prognostic subtypes and key biological mechanisms in MM. The proposed framework provides a scalable and biologically interpretable approach that may support improved risk stratification and the identification of therapeutic targets in multiple myeloma.

Introduction

Multiple myeloma (MM) is a genetically and clinically diverse malignancy of plasma cells that accounts for approximately 10% of all hematologic cancers. It is characterized by the clonal expansion of malignant plasma cells in the bone marrow, leading to bone destruction, immunosuppression, and a range of systemic complications, including anemia, hypercalcemia, and renal failure. [1,2] MM arises from a complex interplay among genetic alterations, epigenetic regulation, and microenvironmental factors.

Landmark studies have defined molecular subtypes of MM based on recurrent chromosomal translocations involving the immunoglobulin heavy-chain (IgH) locus, including t (11;14) (q13; q32), t (4;14) (p16; q32), and t (14;16) (q32; q23), as well as hyperdiploidy characterized by the trisomy of odd-numbered chromosomes. Each subtype is associated with distinct gene expression profiles and clinical outcomes. For example, t(4;14) is linked with poor prognosis because of the overexpression of FGFR3 and MMSET, whereas t(11;14) is generally associated with favorable outcomes and the overexpression of CCND1 [3–5]. More recently, LY6E has been proposed as a prognostic biomarker correlated with aggressive disease and osteoclastogenesis, revealing immune-microenvironmental regulation in MM. [2]. Understanding the biological basis of this heterogeneity is essential for improving prognostic accuracy and developing personalized therapies.

To fully exploit the molecular complexity of MM, computational biology provides a powerful framework for integrating multiomics data and clinical variables. Machine learning and deep learning models have

been successfully applied to patient stratification and outcome prediction across multiple cancer types, including colon and breast cancer. [6–8]. Furthermore, computational modeling of genomic signatures, such as mutations, copy number variations, and chromosomal abnormalities, has shown promise for predicting treatment response and mechanisms of resistance in relapsed or refractory MM patients. [9,10]. These in silico approaches enable the simulation of drug effects on patient-specific molecular networks, paving the way toward individualized therapeutic strategies. [11].

Recent advances integrating bulk and single-cell transcriptomic data have identified prognostically significant cellular subtypes and constructed predictive models that outperform traditional gene-level approaches. [12]. For example, pathway-based modeling techniques such as ssGSEA and GSVA have enabled the development of robust prognostic tools that incorporate immune and signaling pathway activity. [13]. Adapting these approaches to MM could facilitate the construction of survival risk models that better reflect the interplay among the genomic, transcriptomic, and epigenetic layers.

Despite therapeutic progress, including the use of proteasome inhibitors, immunomodulatory agents, and monoclonal antibodies, MM remains incurable, mainly due to tumor heterogeneity, acquired drug resistance, and relapse. [1].

Here, we present a dual-path computational pipeline that integrates mRNA, miRNA, and DNA methylation data to identify survival risk subgroups and construct a robust predictive model. Our objective was to identify prognostic subtypes and key biomarkers associated with disease progression and survival by leveraging deep learning–based dimensionality reduction, Lasso-Cox survival modeling, and systems biology-driven pathway interpretation. This integrative strategy aims to enhance the understanding of MM molecular subtypes and guide personalized therapeutic decision-making.

Results

The dataset description is provided in Table 1.

Table 1
An overview of the data used is presented here.

Subgroup	Patients (n)	Events (n)	% Censored	Median Survival (months)
MY	88	26	70.50%	38.3
CD1	25	11	56.00%	46.9
CD2	44	17	61.40%	33.7
HY	86	32	62.80%	39.7
LB	59	20	66.10%	44.8
MF	34	15	55.90%	38.3
MS	80	44	45.00%	29.9
PR	32	23	28.10%	17.8
Total	368	98	73.40%	39.5

Table 2
An overview of the clinical data is presented here.

Category	Value
Total Number of Patients	368
Number of Events (Death/Event)	98 (26.6%)
Number of Censored	270 (73.4%)
Survival Time (months)	
Minimum	0.1
Maximum	69.24
Median	39.5
Mean	41.1
Standard Deviation	17.6
Subgroups	
Number of Subgroups	8
Subgroup Names	MY, CD1, CD2, HY, LB, MF, MS, PR
Most Common Subgroup	MY" (88 patients, 23.9%)."
Least Common Subgroup	CD2" (44 patients, 12.0%).

The dataset included 559 samples, as shown in Table 1, which displays the frequency with which the final samples were selected for analysis.

2.1. Feature Transformation via a Deep Learning Framework

A dataset comprising 559 multiple myeloma samples served as input for an autoencoder. The matrices scaled to unit norms were combined sample wise to form a unified matrix. The encoder employed two hidden layers with 5,000 and 1,000 nodes; the decoder mirrored this structure, with layers of 1,000 and 5,000 nodes. The model was built via Keras (https://github.com/fchollet/keras) in Python. The autoencoder architecture is depicted in Fig. 3.

2.2. Survival-associated features and segmentation

The GSE2658 dataset was used to collect and preprocess 559 samples with RNA-Seq and clinical data. An autoencoder reduces the number of features to 1000 in the bottleneck layer. These features were fed into a univariate Lasso-Cox model, which identified 30 features linked to survival with significant log-rank p values (< 0.05). These genes were clustered into two groups via k-means and optimized via the C-index. Figure 4 shows Kaplan–Meier curves clearly separating the low- and high-risk groups.

2.3. DEG

After dimensionality reduction techniques and survival analysis were applied, distinct survival-associated groups were identified. Specifically, samples were categorized into high- and low-risk groups, regardless of subtype classification.

In this study, differential gene expression analysis was used to identify differences in gene expression across these groups. The differentially expressed genes (DEGs) were identified via the EBayes method implemented in the Limma package. [14,15]. DEGs in each group with an adjusted p value < 0.05 were subsequently identified based on high- and low-risk patient states. For genes represented by multiple probes, the mean expression value was calculated. On the basis of the analysis, as specified in Fig. 5, the genes are considered probe IDs. These elements are mocked and eventually reported as dysregulated genes.

As presented in Supplementary Table S1, of the 54677 probes examined, 194 + 74 (downregulated and upregulated) genes were identified as significantly differentially expressed on the basis of an adjusted p value < 0.05. These genes are listed in Supplementary Table S2.

2.4. Enrichment analysis

Pathway enrichment analysis via Enrichr identified multiple biologically relevant signatures in the MM cohort, shedding light on key aspects of MM pathogenesis and potential therapeutic vulnerabilities. The

results of the gene enrichment analysis for the selected genes are presented in Fig. 6 and supplementary E1.

The resulting pathway and drug signature enrichment profile revealed a compact and biologically coherent landscape, which converges on four principal domains: (1) dependence on the bone marrow niche, (2) genomic instability and replication stress driven by DNA repair defects, (3) activation of oncogenic survival pathways alongside adaptation to oxidative stress, and (4) metabolic dependencies and druggable vulnerabilities. Each domain is summarized below with direct literature support and translational implications. Enrichment analyses revealed that prognostic risk in multiple myeloma patients is driven by coordinated alterations across the bone marrow microenvironment, the DNA damage response, oncogenic survival signaling, and cellular metabolism. High-risk disease is characterized by disrupted microenvironmental interactions, defective homologous recombination repair involving BRCA2–RAD51 and TP53 dysregulation, and compensatory activation of ATR-mediated stress signaling. Concurrent enrichment of the PI3K–Akt and JAK–STAT pathways, together with signatures of glutamine and lipid metabolism dependence, highlighted convergent survival and metabolic programs. Drug signature analyses revealed that DNA damage response inhibition, glutaminase blockade, JAK–STAT targeting, and fatty acid–binding protein inhibition are actionable vulnerabilities in high-risk myeloma.

2.4.1. Bone marrow microenvironment and osteogenic niches

The enrichment of osteocyte, osteoblast, and common lymphoid progenitor signatures underscores the central role of the marrow microenvironment in MM biology. Malignant plasma cells engage osteoblastic and osteoclastogenic programs and exploit marrow stromal signaling to promote survival, niche retention, and bone destruction; osteocytes produce factors (e.g., RANKL and sclerostin) that further skew bone remodeling and foster tumor expansion. [16,17]. Such tumor–stroma reciprocity not only underlies MM-associated osteolysis but also supports cytokine networks (IL-6, IGF-1) that sustain malignant clones, highlighting the microenvironment as both a disease driver and a therapeutic target [16].

2.4.2. Genomic instability, replication stress, and defective homologous-repair signaling

Pathway enrichment for TP53 regulation, impaired BRCA2–RAD51 interactions, ATR activation, and alternative homology-directed repair (single-strand annealing) points to pervasive DNA damage response (DDR) perturbation and replication stress in MM. Loss or dysfunction of p53 (del(17p) and/or TP53 mutation) is a recurrent, high-risk lesion associated with clonal evolution and poor outcomes. [18], [19]. Impaired BRCA2–RAD51 function and HRR defects increase reliance on compensatory DDR pathways (e.g., ATR/CHK1) and error-prone repair, creating exploitable synthetic lethal interactions. Indeed, preclinical data show that ATR inhibition preferentially kills MM cells with ongoing replication stress and

potentiates alkylator activity, suggesting that DDR inhibitors are promising agents for treating genomically unstable MM subsets. [20].

2.4.3. Oncogenic PI3K–Akt signaling and oxidative stress adaptation

The enrichment of the PI3K–Akt signaling pathway corroborates its central role as a prosurvival axis in MM. The pathway is activated both intrinsically and by marrow-derived cytokines (e.g., IL-6), driving proliferation, anti-apoptosis, and drug resistance [21]. PI3K pathway activation furthermore intersects with mTOR and metabolic circuits, reinforcing anabolic/antiapoptotic programs [21]. The concomitant enrichment of LOXL4/oxidative stress and proteostasis-related processes is consistent with the high proteotoxic and oxidative burdens (due to massive immunoglobulin production) of MM cells. MM cells exhibit adaptive antioxidant and proteostasis responses that can be therapeutically targeted, and PI3K–Akt pathway inhibition has shown preclinical efficacy, particularly in combination regimens. [21].

2.4.4. Metabolic dependencies and druggable vulnerabilities (CB-839, JAK/STAT, FABP inhibitors)

Drug signature enrichment highlights several actionable metabolic and signaling dependencies:

- **Glutaminase inhibition (CB-839/telaglenastat)**: CB-839 signature enrichment reflects the reliance of MM cells on glutamine metabolism. Preclinical work has shown that GLS inhibition depletes α-ketoglutarate and reduces MM cell viability and that CB-839 potentiates the efficacy of proteasome inhibition, HDAC inhibitors, and DDR-targeting agents in model systems [22,23].
- **JAK–STAT pathway (ruxolitinib down)**: The downregulated ruxolitinib signature is associated with hyperactive JAK–STAT signaling in the cohort, which is consistent with cytokine-driven STAT activation (IL-6/JAK axis) that supports MM survival and therapy resistance. Although single-agent JAK inhibition has shown limited clinical benefit, integrating JAK blockade into multimodal regimens remains rational [23].
- **Lipid metabolism/FABP inhibition (BMS309403 downregulation)**: Downregulation of the BMS309403 signature and enrichment of FABP-related genes point to lipid-metabolic dependencies. Recent functional studies have demonstrated that inhibition of fatty acid-binding proteins (e.g., with BMS309403 or SBFI-26) disrupts MM cell proliferation, mitochondrial function, and MYC signaling in vitro and in some in vivo models [24].

In conclusion, the Enrichr profile synthesizes four interlocking hallmarks of MM in this cohort—microenvironmental dependence, genomic instability/replication stress, oncogenic survival signaling, and metabolic/druggable dependencies—supporting a multiaxis therapeutic strategy in which metabolic modulation, DDR inhibition, and PI3K/JAK pathway targeting are rationally combined with marrow-niche-directed approaches.

Discussion

Multiple myeloma (MM) is a hematologic malignancy driven by profound genetic and microenvironmental heterogeneity. In the present study, we leveraged a deep learning-based autoencoder combined with survival modeling to perform unsupervised stratification of MM patients via large transcriptomic datasets. This novel computational approach enables clear demarcation of prognostically distinct high-risk and low-risk clusters with significant survival differences, independent of traditional staging systems such as the International Staging System (ISS) or cytogenetic risk groupings —including those based on t(4;14), t(11;14), and hyperdiploidy. These findings align with the enhanced performance of deep learning models over conventional methods in hematologic malignancies and solid tumors, underscoring the value of advanced machine learning in robust patient stratification. [21,25,26].

The differential expression analysis between risk groups revealed that 268 genes were enriched in hematopoietic dysfunction and oxygen transport pathways, which is consistent with MM-associated anemia and bone marrow suppression. Enrichr-based pathway analysis highlighted the critical role of the bone marrow microenvironment—including osteocytes, osteoblasts, and common lymphoid progenitors —in MM pathogenesis. This finding aligns with an extensive body of evidence demonstrating that malignant plasma cells rely on stromal and osteogenic interactions via IL-6, IGF-1, RANKL, and sclerostin to drive proliferation, survival, and bone disease, supporting the therapeutic targeting of microenvironmental axes (e.g., anti-RANKL or anti-sclerostin agents) in combination regimens. [27–29].

Concurrently, the enrichment of DNA damage response (DDR) pathways—specifically disrupted TP53 function, BRCA2–RAD51 interaction deficits, and ATR-mediated replication stress responses—reveals pervasive genomic instability, a known hallmark of high-risk MM. TP53 deletion and mutation are among the strongest adverse prognostic markers in MM, and their presence significantly drives clonal evolution, chemoresistance, and early relapse [30,31]. BRCA2–RAD51 dysfunction indicates homologous recombination repair (HRR) deficiency, which can be exploited therapeutically via synthetic lethal approaches such as the use of PARP or ATR inhibitors. Preclinical studies have shown promising antimyeloma activity for these agents, especially in HRR-deficient and p53-impaired MM models. [32–34].

Moreover, our analysis highlighted the activation of oncogenic PI3K–Akt signaling and adaptive oxidative stress pathways. PI3K–Akt activation, often driven by cytokine stimulation from the bone marrow microenvironment, supports MM cell survival, growth, and resistance to apoptosis. Targeting this axis with inhibitors such as perifosine has demonstrated preclinical efficacy in MM, and combination strategies—particularly those incorporating proteasome inhibitors—show further promise. [21,25]. The concurrent enrichment of oxidative stress and proteostasis signatures underscores the cellular stress associated with copious immunoglobulin production in plasma cells. Therapeutic strategies that exacerbate proteotoxic stress (e.g., proteasome inhibitors) while inhibiting survival pathways may yield synergistic cytotoxicity. [35,36].

Drug signature enrichment revealed metabolic vulnerabilities, including glutaminolysis dependency (CB-839/Telaglenastat), reliance on JAK–STAT signaling (ruxolitinib), and altered lipid metabolism via fatty acid–binding proteins. Glutaminase inhibition has shown efficacy in multiple myeloma models by disrupting mitochondrial function and sensitizing cells to proteasome and HDAC inhibitors. [23,37]. While clinical trials are ongoing, these findings support metabolic targeting as a viable therapeutic avenue. FABP inhibition is emerging as a novel strategy, with preclinical data demonstrating disruptions in cell proliferation, MYC signaling, and mitochondrial metabolism upon the targeting of FABP pathways in MM [38]. These metabolic dependencies may complement DDR or signaling pathway targeting to overcome adaptive resistance mechanisms.

From a clinical perspective, our integrative computational framework offers three substantial contributions: first, it enables survival stratification that transcends traditional cytogenetic subtypes; second, it unravels key mechanistic pathways—DDR deficiency, PI3K–Akt signaling, and metabolic reprogramming—that drive poor outcomes; and third, it nominates druggable targets (glutaminase, FABPs, ATR, and JAK–STAT) for biomarker-driven therapeutic interventions. This aligns with the precision oncology goal of tailoring treatment strategies to dynamic molecular vulnerabilities rather than static clinical features. [39].

However, several limitations must be considered. The reliance on retrospective bulk transcriptomic datasets limits the resolution of clonal and microenvironmental heterogeneity; integrating single-cell RNA sequencing would enhance the understanding of intratumoral diversity and its interactions with the environment. [40]. The black-box nature of autoencoders also complicates interpretability, necessitating protein-level validation—e.g., via immunohistochemistry, phospho-protein assays, or functional DDR assays—to confirm the biological relevance of computationally derived features. Future studies should incorporate longitudinal sampling and integrate multiomics methods, including proteomics and metabolomics, to capture disease dynamics and evolutionary trajectories. [41]. Importantly, prospective validation in clinical trials is essential to evaluate the predictive capacity and therapeutic utility of the identified risk model.

In summary, our study demonstrates that deep learning-based, multiomics analysis can yield biologically meaningful stratification of MM patients and uncover novel therapeutic vulnerabilities not captured by conventional classification schemes. By aligning computational insights with mechanistic understanding, this framework advances the pursuit of personalized therapy in MM, highlighting actionable pathways for future clinical investigation.

Conclusion

In summary, we presented a novel, unsupervised deep learning framework that integrates multiomics and clinical data to identify prognostic subtypes in multiple myeloma patients. Our results demonstrate that deep learning–derived latent features capture critical biological heterogeneity linked to DNA damage response impairment, metabolic adaptation, and immune microenvironmental variation.

The resulting prognostic model robustly stratifies patient survival across independent cohorts, offering a computationally efficient and biologically interpretable approach to MM risk assessment. Functional analyses revealed the DDR and metabolic pathways as actionable targets, suggesting opportunities for precision therapy.

Future studies integrating proteomic, metabolomic, and single-cell datasets will further enhance model generalizability and translational utility. Ultimately, our findings establish a foundation for AI-driven, biology-informed risk stratification that could guide personalized treatment and clinical trial design in MM patients.

Materials and methods

4.1. Overall pipeline and dataset

This study employed two separate datasets. The Gene Expression Profiles of Multiple Myeloma dataset (GSE2658) was used to identify survival-risk class labels (n = 559), and the second dataset, GSE4581, served as a validation dataset to assess the deep learning model's predictive performance (n = 414). The overall pipeline is illustrated in Fig. 1. Figure 2 presents the study workflow, where Fig. 2A outlines the unsupervised approach for identifying survival-related subgroups, and Fig. 2B shows the downstream pipeline for detecting survival-associated genes.

4.2. Deep Learning Framework for Feature Transformation

An autoencoder is an unsupervised, feed-forward neural network (see Fig. 3) that efficiently compresses and encodes data and then reconstructs the original input from this encoded form, closely approximating it. [42].

Given an input layer that receives data $x = (x_1, \ldots, x_n)$ of dimension n, the autoencoder transforms this input through a series of hidden layers to generate an output x', where x' closely resembles x. It is important to note that both. x and x' share the same dimensionality. [43].

The rectified linear unit (ReLU) is used as the activation function for layer i:

$$Y = f_i(x) = Relu(W_i x + b_i)$$

1

where *x* and *y* are vectors of dimensions *d* and *p*, respectively, W_i denotes a weight matrix of dimensions p, and b_i signifies an intercept vector of dimensionality p.

For an autoencoder consisting of *k* layers, x' is then defined as follows:

$$x' = F_{1\to k}(x) = f_1^{\circ} \ldots f_{k-1}^{\circ} f_k(x)$$

where $f_{k-1}^{\circ} f_k(x) = f_{k-1}(f_k(x))$ is the composing function of f_{k-1} with f_k. The objective of training an autoencoder is to determine the weight vectors W_i of each layer by minimizing the reconstruction loss.

4.3. Features associated with survival and clustering

Dimensionality reduction of features was performed via a deep learning framework, followed by the development of a Lasso-based proportional hazards (Lasso-PH) model for each transformed feature. The features associated with survival were then employed to cluster the samples via the k-means clustering algorithm. The optimal number of clusters was ascertained via the silhouette index, as implemented in the R survcomp package for k-means.

4.4. Confirmation dataset

The GSE4581 dataset, employed as our validation cohort, was processed via the deep autoencoder with identical parameters, followed by the application of the Cox proportional hazards model. The samples were subsequently grouped via the same clustering methodology, marking the commencement of the confirmation analysis.

4.5. Feature Engineering and Pathway Scoring

After clustering, we assessed pathway activity via gene set enrichment analysis (GSEA) and Kyoto Encyclopedia of Genes and Genomes (KEGG) gene sets with Enrichr. The resulting scores served as input features for subsequent modeling and feature engineering.

4.6. Functional Annotation and Interpretation

We used Enrichr to annotate genes and noncoding RNAs related to model performance and to identify enriched pathways. We verified gene relevance by reviewing the literature (2, 8) and by evaluating gene expression in independent MM cohorts.

Declarations

Acknowledgments

We are thankful to Hamadan University of Medical Sciences for its financial support.

Author Contributions Statement

S.S. and H.Ba. conceived and designed the analysis. H.Ba. collected the data. S.S. contributed to analysis tools and performed the analysis. S.S., H.Ba., H. Bas. and S.A. contributed to the interpretation of the results. S.S. and H.B. wrote the manuscript in consultation with all authors.

S.S. Supervision and writing and revising the final version of the paper.

Data availability

The Gene Expression Profiles of Multiple Myeloma dataset (GSE2658) was used to identify survival-risk class labels (n = 559), and GSE4581, served as a validation dataset to assess the deep learning model's predictive performance (n = 414).

Ethics approval and consent to participate

This study used publicly available datasets (GEO: GSE2658 and GSE4581). All data were deidentified, and no new human participants were involved. Therefore, ethics approval and informed consent were not needed.

Competing interests

The authors declare no competing interests.

Funding

The author received No Funding for this work.

Consent to publish

Not applicable

References

1. Bashiri, H., Tabatabaeian, H. & Autophagy A Potential Therapeutic Target to Tackle Drug Resistance in Multiple Myeloma. *Int. J. Mol. Sci.* **24** https://doi.org/10.3390/ijms24076019 (2023).
2. Shi, M. et al. LY6E as a new prognostic biomarker of multiple myeloma-related bone disease. *Sci. Rep.* **15**, 11431. https://doi.org/10.1038/s41598-025-91413-1 (2025).
3. Zhan, F. et al. The molecular classification of multiple myeloma. *Blood* **108**, 2020–2028. https://doi.org/10.1182/blood-2005-11-013458 (2006).
4. Cardona-Benavides, I. J., de Ramón, C. & Gutiérrez, N. C. Genetic Abnormalities in Multiple Myeloma: Prognostic and Therapeutic Implications. *Cells* **10** https://doi.org/10.3390/cells10020336 (2021).
5. Fonseca, R. et al. Clinical and biologic implications of recurrent genomic aberrations in myeloma. *Blood* **101**, 4569–4575. https://doi.org/10.1182/blood-2002-10-3017 (2003). https://doi.org/
6. Salimy, S. et al. A deep learning-based framework for predicting survival-associated groups in colon cancer by integrating multi-omics and clinical data. *Heliyon* 9, e17653 (2023). https://doi.org/10.1016/j.heliyon.2023.e17653
7. Tapak, L. et al. Identification of Prognostic Biomarkers for Breast Cancer Metastasis Using Penalized Additive Hazards Regression Model. *Cancer Inf.* **22**, 11769351231157942. https://doi.org/10.1177/11769351231157942 (2023).

8. Habibzadeh, G. et al. Identification of lncRNA associated with the SERPINE1 gene in colorectal cancer through TGF-β pathway. *Comput. Biol. Med.* **190**, 110037. https://doi.org/10.1016/j.compbiomed.2025.110037 (2025).
9. Paulus, A. et al. Computational Modelling of Multiple Myeloma Patient Genomic Signatures to Predict Treatment Outcome. *Blood* 132, https://doi.org/ (1911). (2018) https://doi.org/10.1182/blood-2018-99-119574
10. Kamal, M. et al. Single-cell proteomic analysis reveals Multiple Myeloma heterogeneity and the dynamics of the tumor immune microenvironment in precursor and advanced states. *Neoplasia* **66**, 101189. https://doi.org/10.1016/j.neo.2025.101189 (2025).
11. Chaudhary, K., Poirion, O. B., Lu, L. & Garmire, L. X. Deep Learning-Based Multi-Omics Integration Robustly Predicts Survival in Liver Cancer. *Clin. Cancer Res.* **24**, 1248–1259. https://doi.org/10.1158/1078-0432.Ccr-17-0853 (2018).
12. Wang, Y. et al. Single-cell sequencing analysis of multiple myeloma heterogeneity and identification of new theranostic targets. *Cell. Death Dis.* **15**, 672. https://doi.org/10.1038/s41419-024-07027-4 (2024).
13. Su, K. et al. Pan-cancer analysis of pathway-based gene expression pattern at the individual level reveals biomarkers of clinical prognosis. *Cell. Rep. Methods*. **1** https://doi.org/10.1016/j.crmeth.2021.100050 (2021).
14. Smyth, G. K. Linear models and empirical bayes methods for assessing differential expression in microarray experiments. *Stat. Appl. Genet. Mol. Biol.* **3**, Article3 (https://doi.org/10.2202/1544-6115.1027 (2004).
15. Maghsoudloo, M., Azimzadeh Jamalkandi, S., Najafi, A. & Masoudi-Nejad, A. Identification of biomarkers in common chronic lung diseases by co-expression networks and drug-target interactions analysis. *Mol. Med.* **26**, 9. https://doi.org/10.1186/s10020-019-0135-9 (2020).
16. Mukkamalla, S. K. R. & Malipeddi, D. Myeloma Bone Disease: A Comprehensive Review. *Int. J. Mol. Sci.* **22** https://doi.org/10.3390/ijms22126208 (2021).
17. Anloague, A., Delgado-Calle, J. & Osteocytes New Kids on the Block for Cancer in Bone Therapy. *Cancers* **15**, 2645 (2023).
18. Gaballa, S. et al. Outcomes in patients with multiple myeloma with TP53 deletion after autologous hematopoietic stem cell transplant. *Am. J. Hematol.* **91**, E442–447. https://doi.org/10.1002/ajh.24487 (2016).
19. Martello, M. et al. Clonal and subclonal TP53 molecular impairment is associated with prognosis and progression in multiple myeloma. *Blood Cancer J.* **12**, 15. https://doi.org/10.1038/s41408-022-00610-y (2022).
20. Botrugno, O. A. et al. ATR addiction in multiple myeloma: synthetic lethal approaches exploiting established therapies. *Haematologica* **105**, 2440–2447. https://doi.org/10.3324/haematol.2018.215210 (2020).

21. Ikeda, H. et al. PI3K/p110δ is a novel therapeutic target in multiple myeloma. *Blood* **116**, 1460–1468. https://doi.org/10.1182/blood-2009-06-222943 (2010).
22. Shen, Y. A. et al. Inhibition of glutaminolysis in combination with other therapies to improve cancer treatment. *Curr. Opin. Chem. Biol.* **62**, 64–81. https://doi.org/10.1016/j.cbpa.2021.01.006 (2021).
23. Varghese, S. et al. The Glutaminase Inhibitor CB-839 (Telaglenastat) Enhances the Antimelanoma Activity of T-Cell-Mediated Immunotherapies. *Mol. Cancer Ther.* **20**, 500–511. https://doi.org/10.1158/1535-7163.Mct-20-0430 (2021).
24. Farrell, M. et al. Targeting the fatty acid binding proteins disrupts multiple myeloma cell cycle progression and MYC signaling. *Elife* **12** https://doi.org/10.7554/eLife.81184 (2023).
25. Hideshima, T. et al. Perifosine, an Oral Bioactive Novel Alkyl-Phospholipid, Inhibits Akt and Induces In Vitro and In Vivo Cytotoxicity in Human Multiple Myeloma (MM) Cells. *Blood* **106**, 250–250. https://doi.org/10.1182/blood.V106.11.250.250 (2005).
26. Li, C. et al. Targeting Glutaminolysis to Treat Multiple Myeloma: An In Vitro Evaluation of Glutaminase Inhibitors Telaglenastat and Epigallocatechin-3-gallate. *Anticancer Agents Med. Chem.* **23**, 779–785. https://doi.org/10.2174/1871520622666220905142338 (2023).
27. Silbermann, R. & Roodman, G. D. Myeloma bone disease: Pathophysiology and management. *J. Bone Oncol.* **2**, 59–69. https://doi.org/10.1016/j.jbo.2013.04.001 (2013).
28. Roodman, G. D. Pathogenesis of myeloma bone disease. *Leukemia* **23**, 435–441. https://doi.org/10.1038/leu.2008.336 (2009).
29. Huang, S. Y. et al. Denosumab Versus Zoledronic Acid in Bone Disease Treatment of Newly Diagnosed Multiple Myeloma: An International, Double-Blind, Randomized Controlled Phase 3 Study-Asian Subgroup Analysis. *Adv. Ther.* **37**, 3404–3416. https://doi.org/10.1007/s12325-020-01395-x (2020).
30. Chng, W. J. et al. IMWG consensus on risk stratification in multiple myeloma. *Leukemia* **28**, 269–277. https://doi.org/10.1038/leu.2013.247 (2014).
31. Walker, B. A. et al. Intraclonal heterogeneity is a critical early event in the development of myeloma and precedes the development of clinical symptoms. *Leukemia* **28**, 384–390. https://doi.org/10.1038/leu.2013.199 (2014).
32. Herrero, A. B. & Gutiérrez, N. C. Targeting Ongoing DNA Damage in Multiple Myeloma: Effects of DNA Damage Response Inhibitors on Plasma Cell Survival. *Front. Oncol.* **7**, 98. https://doi.org/10.3389/fonc.2017.00098 (2017).
33. Saitoh, T. & Oda, T. D. N. A. Damage Response in Multiple Myeloma: The Role of the Tumor Microenvironment. *Cancers* **13**, 504 (2021).
34. Li, L. et al. Combined MEK1/2 and ATR inhibition promotes myeloma cell death through a STAT3-dependent mechanism in vitro and in vivo. *Br. J. Haematol.* **205**, 2338–2348. https://doi.org/10.1111/bjh.19796 (2024).
35. Obeng, E. A. et al. Proteasome inhibitors induce a terminal unfolded protein response in multiple myeloma cells. *Blood* **107**, 4907–4916. https://doi.org/10.1182/blood-2005-08-3531 (2006).

36. Cui, Y., Wang, F. & Fang, B. Mitochondrial dysfunction and drug targets in multiple myeloma. *J. Cancer Res. Clin. Oncol.* **149**, 8007–8016. https://doi.org/10.1007/s00432-023-04672-8 (2023).
37. Qiu, Q. et al. Targeting glutaminase1 and synergizing with clinical drugs achieved more promising antitumor activity on multiple myeloma. *Oncotarget* **10**, 5993–6005. https://doi.org/10.18632/oncotarget.27243 (2019).
38. Diedrich, C., Maksimos, M. & Azab, A. K. Fatty acid binding proteins in multiple myeloma. *Trends Mol. Med.* **29**, 584–585. https://doi.org/10.1016/j.molmed.2023.05.011 (2023).
39. Rituraj et al. Precision oncology: transforming cancer care through personalized medicine. *Med. Oncol.* **42**, 246. https://doi.org/10.1007/s12032-025-02817-y (2025).
40. Ledergor, G. et al. Single cell dissection of plasma cell heterogeneity in symptomatic and asymptomatic myeloma. *Nat. Med.* **24**, 1867–1876. https://doi.org/10.1038/s41591-018-0269-2 (2018).
41. Salomon-Perzyński, A., Jamroziak, K. & Głodkowska-Mrówka, E. Clonal Evolution of Multiple Myeloma-Clinical and Diagnostic Implications. *Diagnostics (Basel)*. 11. https://doi.org/10.3390/diagnostics11091534 (2021).
42. Bengio, Y. Learning deep architectures for AI. *Found. trends® Mach. Learn.* **2**, 1–127 (2009).
43. Chaudhary, K., Poirion, O. B., Lu, L. & Garmire, L. X. Deep Learning–Based Multi-Omics Integration Robustly Predicts Survival in Liver Cancer. *Clin. Cancer Res.* **24**, 1248–1259. https://doi.org/10.1158/1078-0432.ccr-17-0853 (2018).

Figures

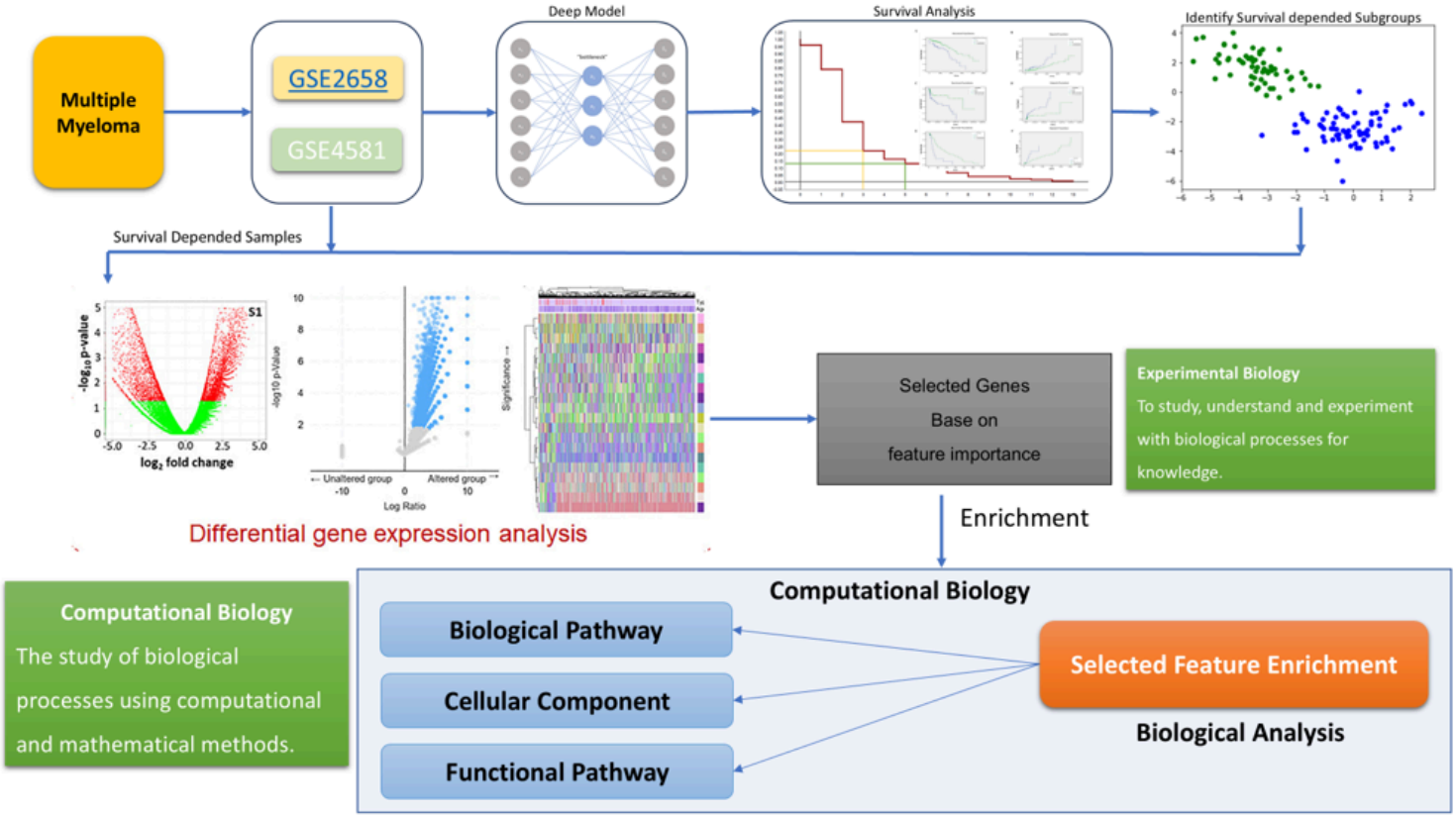


Figure 1

Study pipeline. The overall pipeline, from the probe ID to the functional pathway, is depicted.

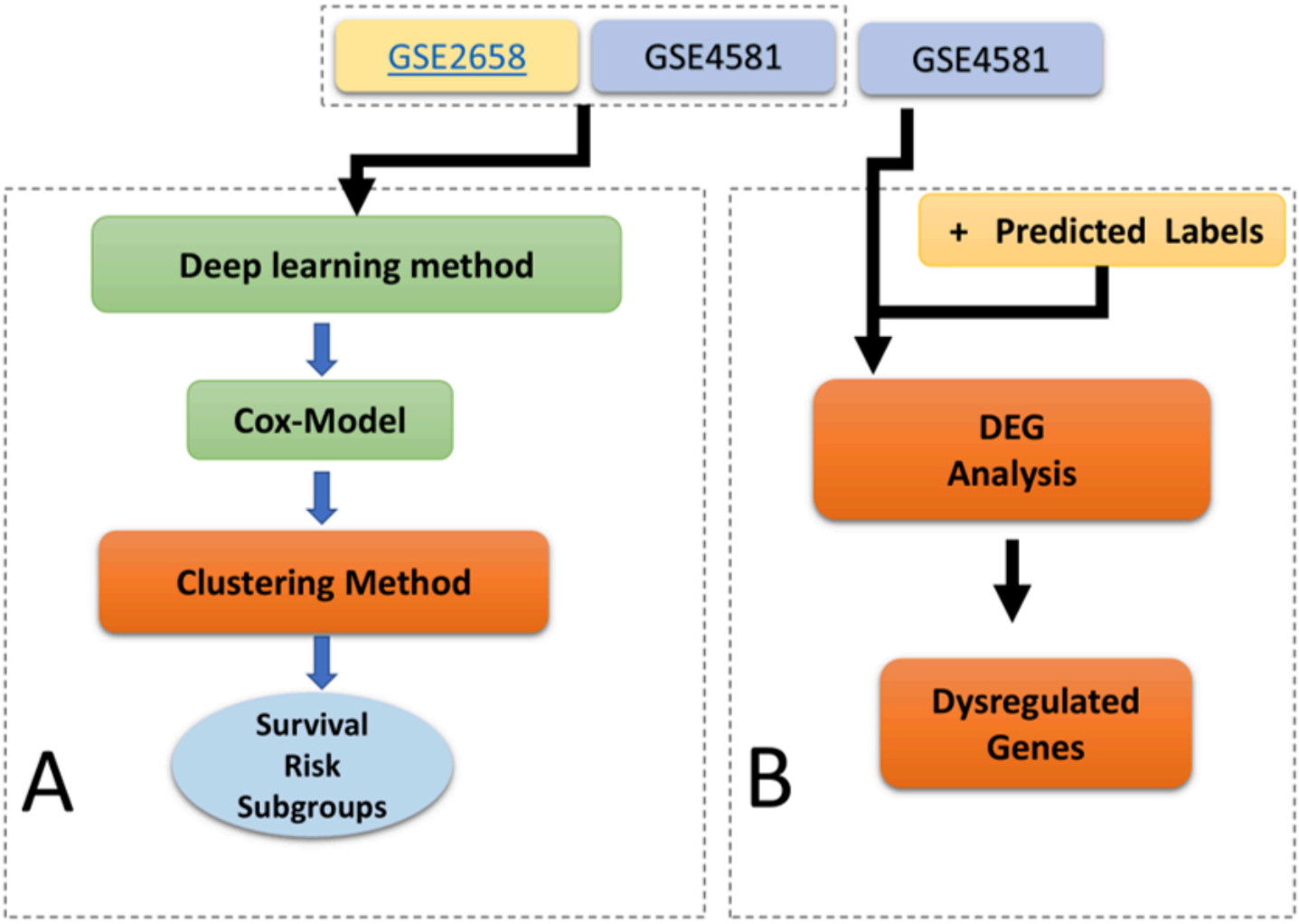


Figure 2

The workflow overview. A. An unsupervised survival analysis pipeline was designed to identify subgroups associated with survival outcomes. B. Pipeline used to identify significant genes from newly clustered (high and low) samples.

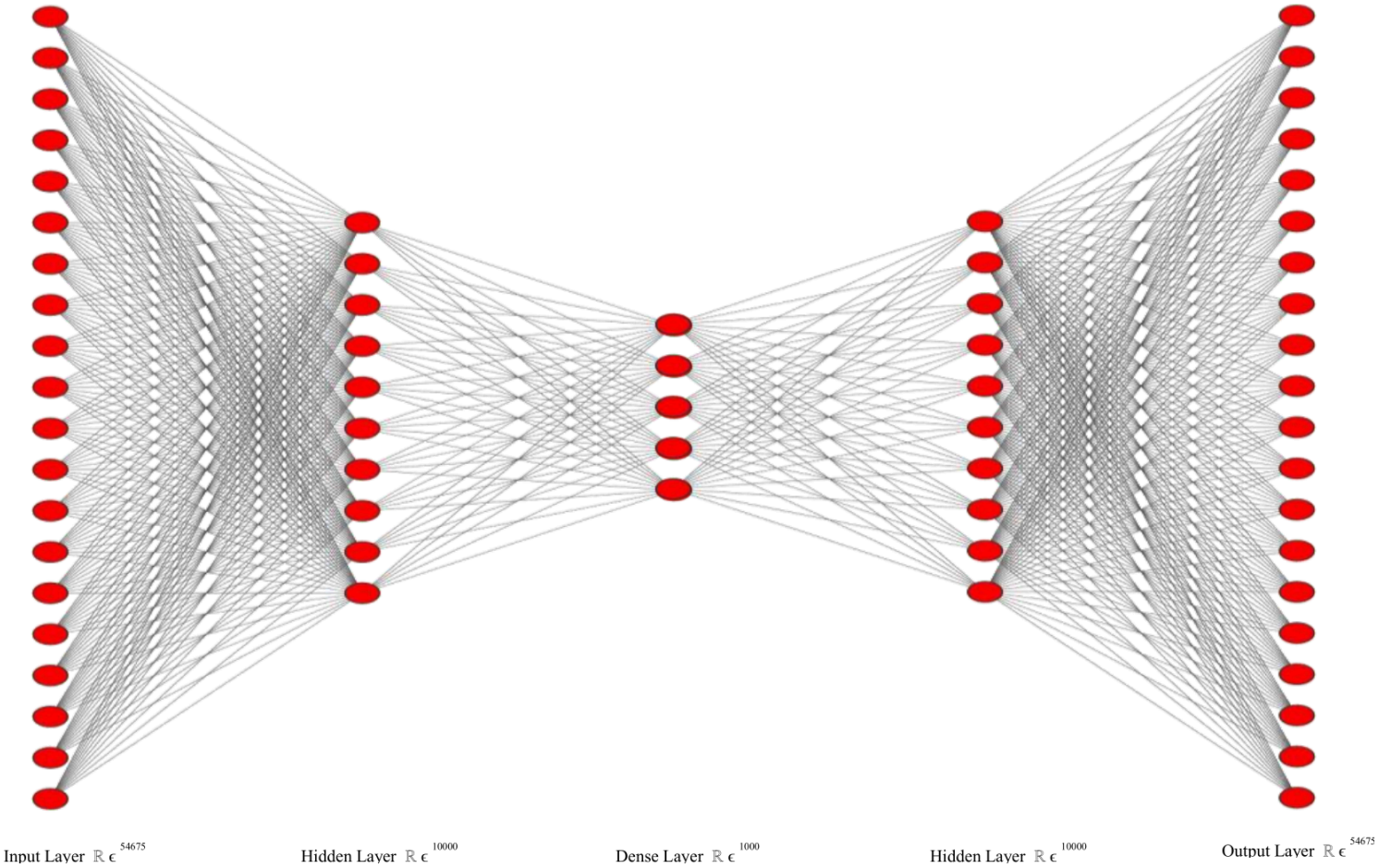


Figure 3

The autoencoder schema is used for dimension reduction.

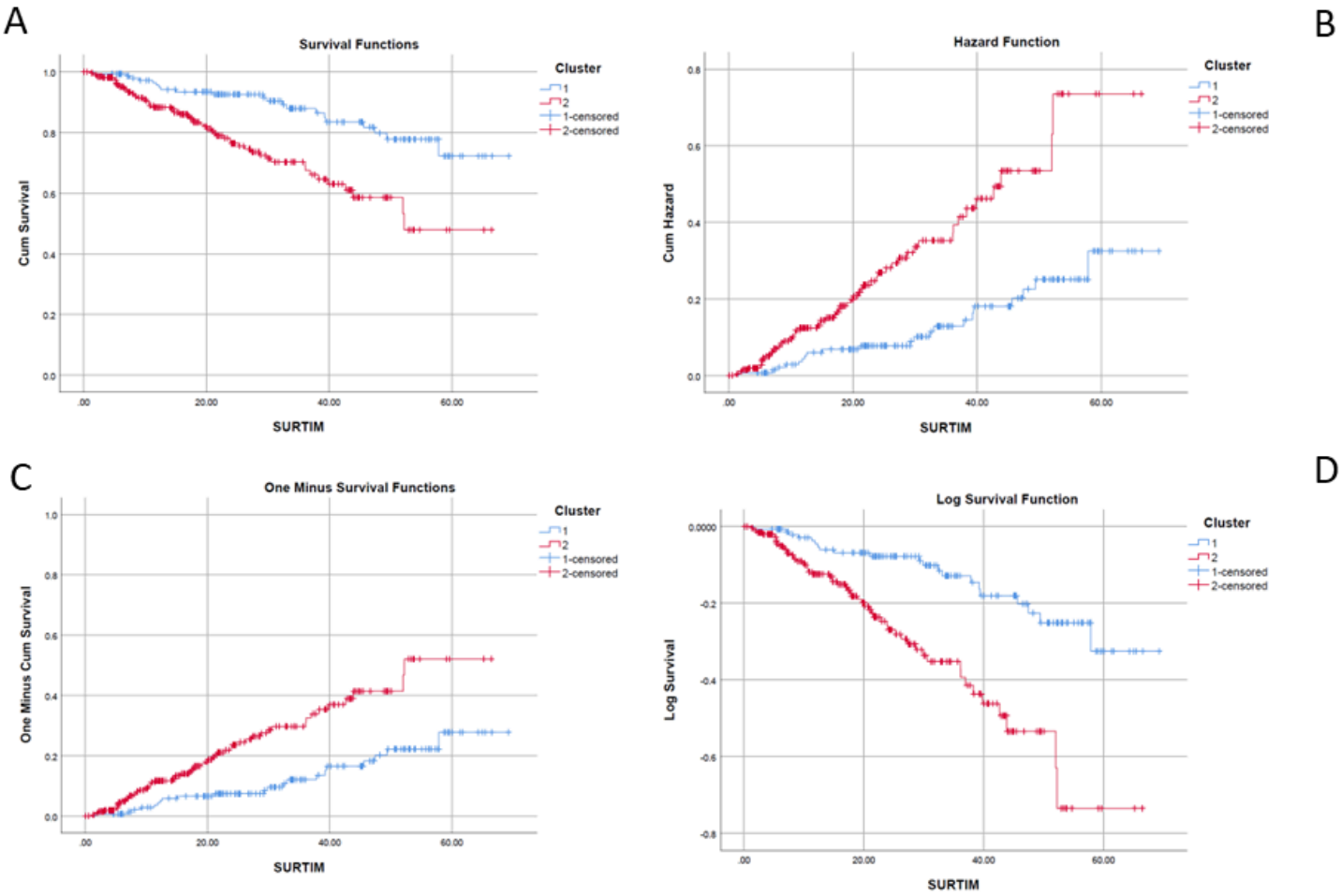


Figure 4

The Kaplan–Meier survival curve is shown, where the blue line represents the low-risk group and the red line represents the high-risk group.

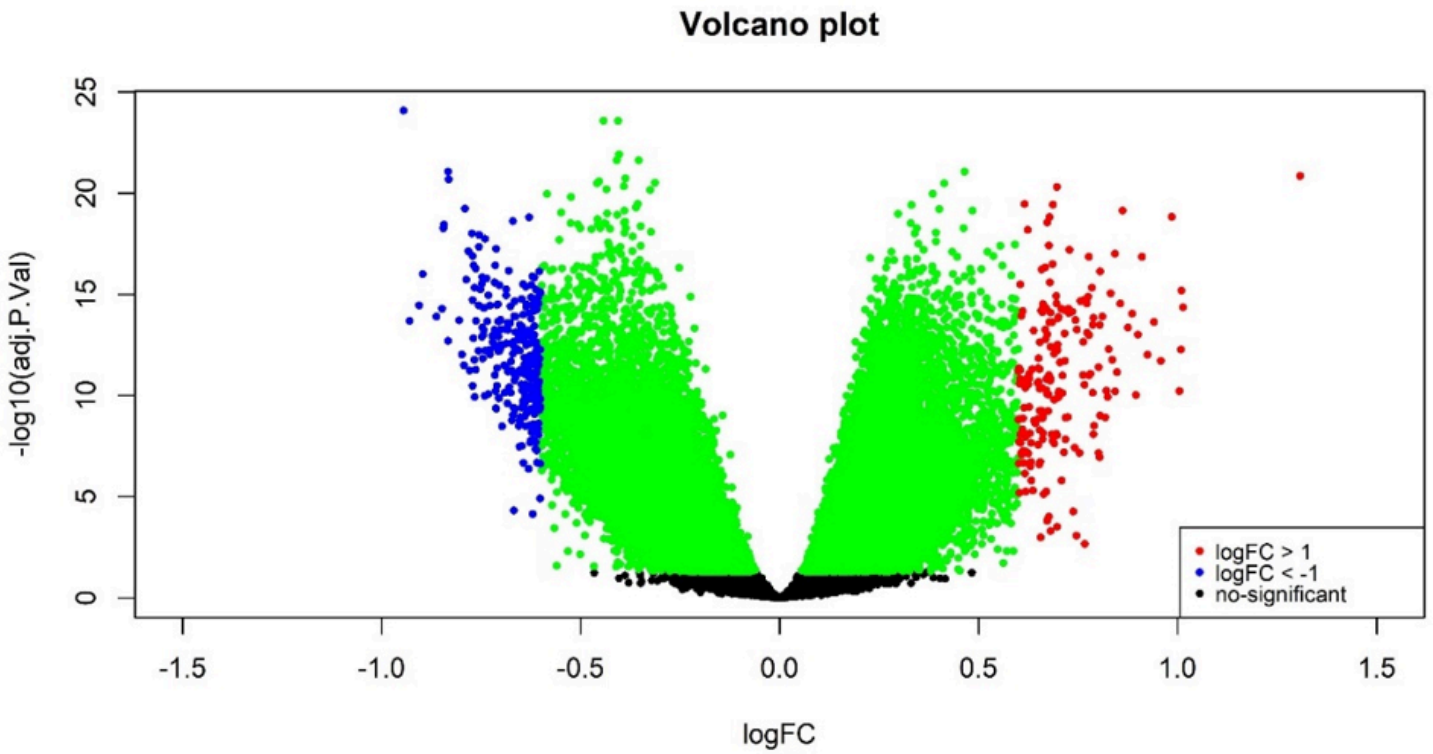
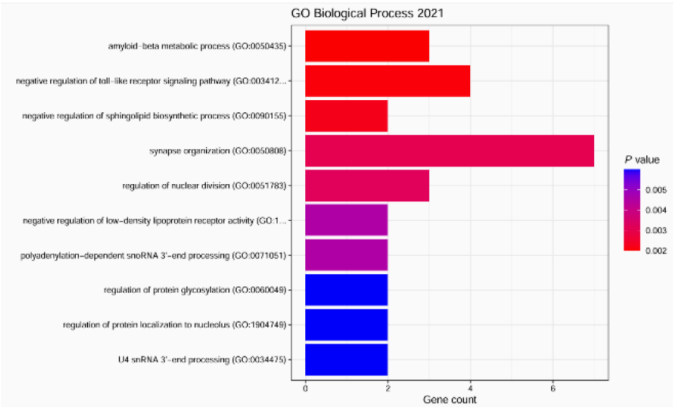


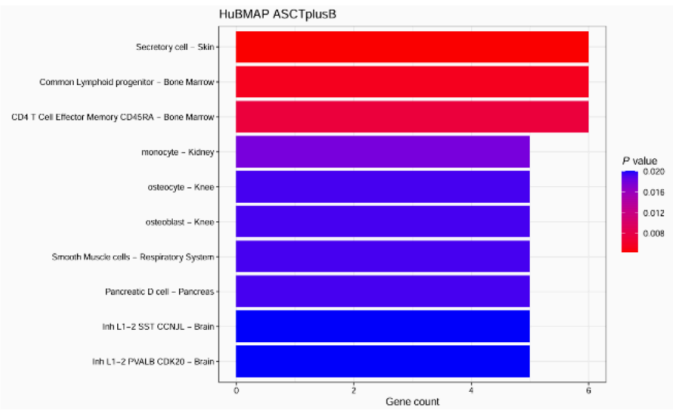
Figure 5

Volcano plot of dysregulated genes in GSE2658. The green dots represent the probes that are significant (p value < 0.05), with logFC < 1 and > -1.

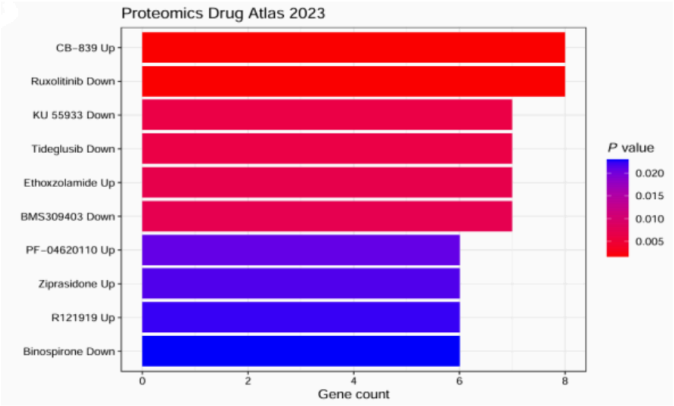
A. GO_Biological Process



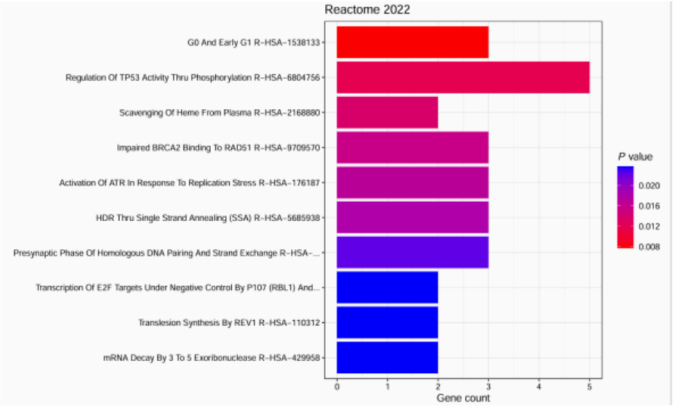
B. HuBMAP_ASCTPlusB



C. Proteomics_Drug Atlas



D. Reactome



E. WikiPathway



Figure 6

Enrichment analysis of the dysregulated genes. (A, B) GO and HuBMAP enrichment analysis of DEGs. (C, D, E) Proteomic, Reactome, and WikiPathway results of the dysregulated genes.